An explicit spectral element method for the acoustic wave equation

Saulo Pomponet Oliveira, CPGG/UFBA

Abstract

We discuss a low-order spectral element method that is explicit in time. This method is compared with the standard finite-difference method for the acoustic wave equation in two space dimensions. Although reduced integration is employed, the method is consistent in the sense that diagonal and stiffness matrices are evaluated with the same integration rule, which is a tensor product of Simpson's rule. To ensure a diagonal mass matrix, the zeros of the weighting functions are taken at the integration points.

Introduction

The finite-element method (FEM) is a numerical technique suitable to problems involving complex geometries and material properties. When applied to time-dependent problems, FEM usually leads to implicit schemes, which require the solution of a linear system at each time step. However, explicit finite-difference methods (FDM) for the wave equation are not severely limited by stability conditions, in contrast to parabolic governing equations. Moreover, FEM and FDM yield similar results. For these reasons (Kelly et al, 1982) FDM is a natural choice for seismic modeling.

To reduce computer processing time and memory requirements, one may consider employing explicit FEM schemes, which in turn depend on the structure of the mass matrix. For instance, consider the following problem involving the one-dimensional wave equation (with dots meaning differentiation with respect to time):

$$\begin{cases} \ddot{p} - \dfrac{\partial^2 p}{\partial x^2} = f & \text{in} \quad]0,1[\times]0,T[\ , \\ p(0,t) = p(1,t) = 0 & , \ t > 0 \ , \\ p(x,0) = 0 & , \ 0 < x < 1 \ , \\ \dot{p}(x,0) = 0 & , \ 0 < x < 1 \ . \end{cases} \tag{1}$$

Given the weighting functions $w_1(x), \ldots, w_m(x)$ satisfying $w_i(0) = w_i(1) = 0$, $1 \le i \le m$, the FEM *semi-discretization in space* approximates p by

$$p_h(x,t) = \sum_{j=1}^{m} p_j(t) w_j(x) \ . \tag{2}$$

Multiply (1) by $w_i(x)$, integrate with respect to x, integrating the second term of the left-hand side by parts:

$$\int_0^1 \ddot{p} w_i \, dx + \int_0^1 \frac{\partial p}{\partial x}\frac{\partial w_i}{\partial x} \, dx = \int_0^1 f w_i \, dx \ . \tag{3}$$

Substituting p by p_h in (3), we find

$$\begin{aligned} \boldsymbol{M}\ddot{\boldsymbol{x}}(t) + \boldsymbol{K}\boldsymbol{x}(t) &= \boldsymbol{F} \ , \\ x_i(t) &= p_i(t) \ , \\ M_{i,j} &= \int_0^1 w_i w_j \, dx \ , \\ K_{i,j} &= \int_0^1 \frac{\partial w_i}{\partial x}\frac{\partial w_j}{\partial x} \, dx \ , \\ F_i &= \int_0^1 f w_i \, dx \ . \end{aligned} \tag{4}$$

Matrices $\boldsymbol{M}$ and $\boldsymbol{K}$ are called *mass* and *stiffness* matrices, respectively. Let $t_0 \le t_1 \le \ldots \le t_n$ be a partition of $[0,T]$ in time steps of length Δt and $x_n = (p_1(t_n), \ldots, p_m(t_n))$. The forward in time, second-order central-difference scheme can be written as

$$\boldsymbol{M}\boldsymbol{x}^{n+1} = \Delta t^2 \boldsymbol{F} + (2\boldsymbol{M} - \Delta t^2 \boldsymbol{K})\boldsymbol{x}^n - \boldsymbol{M}\boldsymbol{x}^{n-1} \ . \tag{5}$$

Note that equations (5) yield an explicit scheme only if the mass matrix $\boldsymbol{M}$ is diagonal, that is, if the weighting functions $w_1(x), \ldots w_m(x)$ are orthogonal:

$$\int_0^1 w_i w_j \, dx = 0 \quad \text{if} \quad i \ne j \ . \tag{6}$$

Lex $x_0 \le x_1 \le \ldots \le x_{m+1}$ be a partition of $[0,1]$ in intervals of length $h = \Delta x$ and w_i be standard interpolation functions (i.e., w_i are piecewise polynomial and $w_i(x_j) = 0$ if $i \ne j$). One can achieve (6) by computing $\boldsymbol{M}$ with integration points at x_j, $j = 1, \ldots m$. This technique is known as *lumping*, since it concentrates mass over the nodes.

A recent method (Komatitsch and Vilotte, 1998) employs Gauss-Lobatto integration points (which are also used as basis points of the weighting functions) to compute all entries of (4). This approach renders orthogonal weighting functions without resorting to selective integration.

The method of Komatitsch and Vilotte fits into the class of *spectral element methods*, which employ high-order orthogonal polynomial weighting functions whose basis (or collocation) points are the same as in the integration rule. These methods represent the state of the art in finite elements for seismic modeling (Carcione et al, 2002).

The goal of this note is to study the low-order version of this method, which is described in the following section. One test problem has an analytical solution, providing us with estimates of the stability condition and the convergence rate. A second example simulates a common source (CS) gather of a non-homogeneous 2D section.

Method

Let $\Omega \subset I\!R^2$ and $\partial\Omega = \Gamma_1 \cup \Gamma_2$. Consider the following initial boundary-value problem:

$$\begin{cases} \ddot{p} - \nabla \cdot (c^2 \nabla p) = f & \text{in} \quad \Omega \times]0, T[\ , \\ p = 0 & \text{on} \quad \Gamma_1 \ , \ t > 0 \ , \\ c^2 \nabla p \cdot \boldsymbol{n} = 0 & \text{on} \quad \Gamma_2 \ , \ t > 0 \ , \\ p(x,y,0) = g_0(x,y) & \text{in} \quad \Omega \ , \\ \dot{p}(x,y,0) = g_1(x,y) & \text{in} \quad \Omega \ . \end{cases} \tag{7}$$

Problem (7) is a model for acoustic waves where $c = c(x,y)$ can be associated with the compressional velocity $V_P = ((\lambda + 2\mu)/\rho)^{1/2}$ for $\mu \approx 0$ (Rivière and Wheeler, 2001; Passos, 2002).

Consider weighting functions $w_1(x,y), \ldots, w_m(x,y)$ satisfying $w_i = 0$ in Γ_1. Proceeding as in (2)-(5), we find

$$\begin{aligned} \boldsymbol{M}\boldsymbol{x}^{n+1} &= \Delta t^2 \boldsymbol{F} + (2\boldsymbol{M} - \Delta t^2 \boldsymbol{K})\boldsymbol{x}^n - \boldsymbol{M}\boldsymbol{x}^{n-1} \ , \\ x_i^n &= p_i(t_n) \ , \\ M_{i,j} &= \iint_\Omega w_i w_j \, d\Omega \ , \\ K_{i,j} &= \iint_\Omega c^2 \nabla w_i \cdot \nabla w_j \, d\Omega \ , \\ F_i &= \iint_\Omega f w_i \, d\Omega \ . \end{aligned} \tag{8}$$

Let us partition Ω into non-overlapping quadrilaterals Ω^e, $e = 1, \ldots n_{el}$. Standard finite-element methods perform a bilinear transformation $F = F_e$ from each *element* Ω^e to the reference domain $\hat{K} = [-1, 1]$, where computations are performed with the aid of an integration rule. In particular, we employ a tensor product of Simpson's rule:

$$\int_{-1}^{1} u(\xi) \, d\xi \approx \sum_{l=1}^{3} A_i u(\xi_l) \ ,$$

$$A_1 = A_3 = \frac{1}{3}, \ A_2 = \frac{4}{3}, \ \xi_1 = -1, \ \xi_2 = 0, \ \xi_3 = 1 \ .$$

Let $J = J(\xi_k, \xi_l)$ be the Jacobian of the transformation F_e and $\hat{w}_i(\xi, \eta) = w_i(x(\xi,\eta), y(\xi,\eta))\,|_{\Omega^e}$. For instance,

$$M_{ij} = \iint_{\Omega^e} w_i w_j \, d\Omega = \int_{-1}^{1} \int_{-1}^{1} \hat{w}_i(\xi,\eta) \hat{w}_j(\xi,\eta) \, |J| \, d\xi d\eta$$

is computed as follows:

$$\tilde{M}_{ij} = \sum_{k=1}^{3} \sum_{l=1}^{3} A_k A_l \hat{w}_i(\xi_k, \xi_l) \hat{w}_j(\xi_k, \xi_l) \, |J(\xi_k, \xi_l)| \ . \tag{9}$$

Although Simpson's rule is less accurate than the standard Gaussian quadrature ($A_{1,2} = 1$ and $\xi_{1,2} = \pm 1/\sqrt{3}$), it has the advantage of including the element nodes in the integration rule, which leads to the same argument of the lumping technique. In one-dimensional problems, Simpson's rule refines lumping with the inclusion of an extra integration point at each interval midpoint.

We define the weighting functions in the reference element using the Lagrange family of degree two for rectangular elements (Zienkiewicz, 1971); that is, $w_k(\xi, \eta) = v_i(\xi) v_j(\eta)$, where the one-dimensional functions $v_i \ (i = 1, 2, 3)$ are given by

$$\begin{aligned} v_1(\xi) &= (\xi - 1)\xi/2 \ , \\ v_2(\xi) &= 1 - \xi^2 \ , \\ v_3(\xi) &= (\xi + 1)\xi/2 \ . \end{aligned} \tag{10}$$

From (9), $\tilde{M}_{ij} = 0$ if $i \neq j$, which allows us to write equations (8) as an explicit scheme.

Simpson's rule is a particular case of Gauss-Lobatto rules (Davis and Rabinowitz, 1984). Komatitsch and Vilotte employed polynomial weighting functions of degree N and considered $N + 1$ Gauss-Lobatto integration points.

Examples

In the first example we consider $\Omega = [0,1] \times [0,1]$, $c = 1$, $f = g_1 = 0$, $\Gamma_2 = \emptyset$, and $g_0(x,y) = \sin(\pi x)\sin(\pi y)$. In this case, the solution of (7) is

$$p(x,y,t) = \sin(\pi x)\sin(\pi y)\cos(\sqrt{2}\pi t) \ . \tag{11}$$

Being an explicit method, (8) is subject to a stability condition which limits the relative sizes of h and Δt. Komatitsch and Vilotte established (in the two-dimensional case) $\Delta t = \mathcal{O}(hN^{1/2})$, but did not provide an upper bound for the ratio $\Delta t/h$.

The numerical experiments are performed in two meshes of $m \times m$ elements, shown in Figure 1. We denote the solutions using the square and non-square meshes by FEM1 and FEM2, respectively, while the finite-difference solutions (in the square mesh) are denoted by FDM. We employ an explicit FDM scheme of second order in time and fourth order in space (Botelho, 1986).

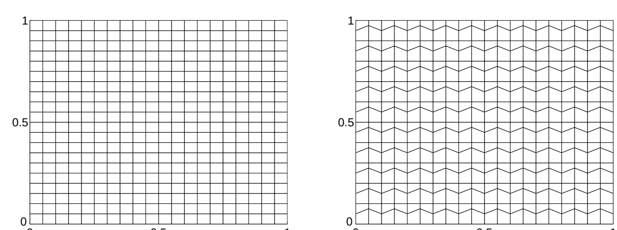

Figure 1: Meshes employed in the first example.

Let us estimate such bound proceeding as follows: for each time step Δt we fix $T = 10$ and solve (7) with progressively smaller values of $h = 1/m$ until the stability condition is violated, i.e., when the error

$$e = \|p_h - p\| = \left(\iint_\Omega (p_h(x,y,T) - p(x,y,T))^2 \, d\Omega \right)^{1/2} \ .$$

becomes suddenly large. Figure 2 shows graphs of Δt against the maximum $h = h(\Delta t)$ for which stability is observed. The resulting curves stand below the line $h = 5\Delta t$, providing an estimate in the form

$$r = \frac{c\Delta t}{h} < \frac{1}{5} \quad .$$

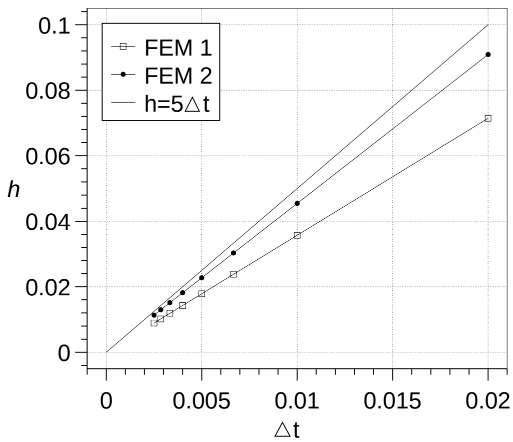

Figure 2: Numerical study of the ratio $\Delta t/h$.

Figure 3 compares the estimate convergence rates of the solutions FEM1, FEM2, and FDM when $T = 1$. The estimate stability condition of FDM is $r \leq 2^{1/2}$ (Kelly et al, 1982). Therefore, FDM admits finer meshes than FEM1,2 under the same time step. Nevertheless, the observed errors FEM1 were significantly lower than FDM. Note that the errors of FDM and FEM2 were similar.

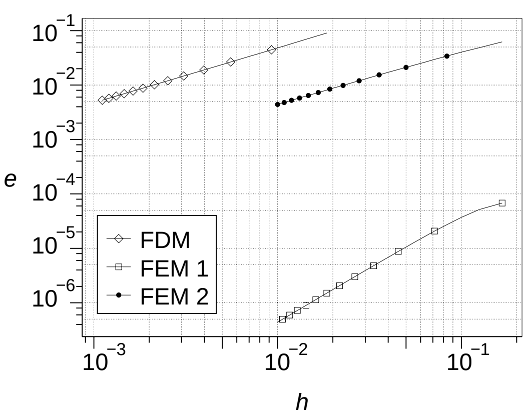

Figure 3: Estimate convergence curves of spectral and finite-difference methods.

The second example simulates of a common source (CS) gather of a 3600m×1200m section composed of two homogeneous layers. The velocities on the upper and lower layers are 2000m/s and 2500 m/s, respectively.

FDM is implemented with absorbing strips of 19 points length, while FEM1 employs a Rayleigh damping strip (Sarma et al 1998) of 4 elements. The shot and the seismometers are located right below the absorbing strips; the layer interface is 400m below the absorbing strips.

Figures 4 and 5 show the synthetic seismograms generated by FEM1 and FDM, respectively.

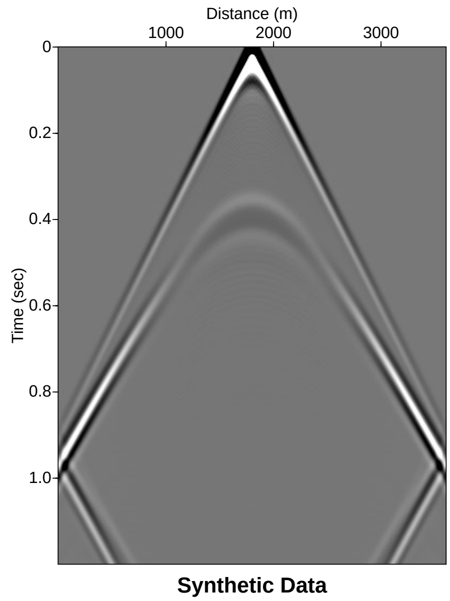

Figure 4: FEM1 CS gather ($\Delta t = 1ms$ and $h = 20m$).

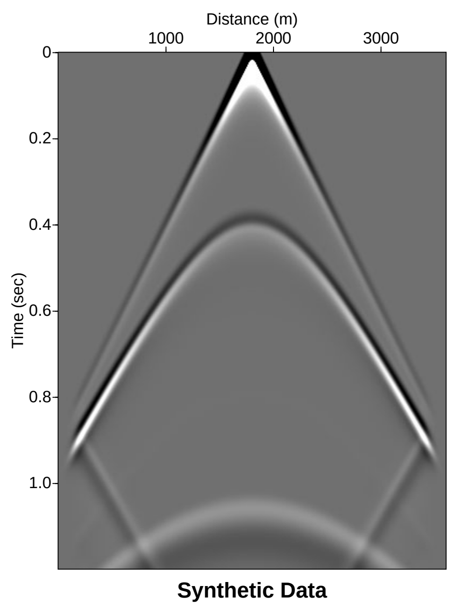

Figure 5: FDM CS gather ($\Delta t = 2ms$ and $h = 10m$).

Conclusions

The low-order version of the spectral element method proposed by Komatitsch and Vilotte reduces to a simple finite-element method that performs computations with Simpson's rule and naturally leads to an explicit scheme.

Numerical studies suggest an estimate stability condition $c\Delta t/h < 1/5$. Although this condition is more restrictive than the finite-difference condition, the spectral element method has shown to be more accurate.

Acknowledgments

The author is supported by the PRODOC fellowship provided by CAPES, Brazil.

References

Botelho, M. A. B., 1986, Modelamento sísmico na bacia do recôncavo usando a técnica de traçamento de raios (in Portuguese). Doctorate thesis, Universidade Federal da Bahia.

Carcione, J., Herman, G. and ten Kroode, A., 2002, Seismic modeling. Geophysics, Vol. 67, p1304-1325

Davis, P. and Rabinowitz, P., 1984, Methods of numerical integration, 2nd. ed. Academic Press, San Diego, CA.

Kelly, K., Alford, R. and Whitmore, N., 1982, Modeling - the forward method. In Jain, K. and Figueiredo, R., Society for Exploration Geophysicists, Tulsa, OK, p91-114

Komatitsch, D. and Vilotte, J.-P., 1998, The spectral element method: an efficient tool to simulate the seismic response of 2D and 3D geological structures. Bulletin of the Seismic Society of America, Vol. 88, p368-392

Passos, G. F. dos, 2002, Modelagem sísmica em meios efetivos simulando reservatórios de hidrocarbonetos (in Portuguese). Master thesis, Universidade Federal da Bahia.

Rivière, B. and Wheeler, M., 2001, Discontinuous finite element methods for acoustic and elastic wave problems. part i: semidiscrete error estimates. Texas Institute for Computational and Applied Mathematics Report 01-02

Sarma, G., Mallick, K. and Gadhinglajkar, V., 1998, Nonreflecting boundary condition in finite-element formulation for an elastic wave equation. Geophysics, Vol. 63, p.1006-1016

Zienkiewicz, O., 1971, The finite element method in engineering science, 2nd. ed. MacGraw Hill, London.